Effects of climate, land cover and topography on soil erosion risk in a semiarid basin of the Andes

CrossMark

P.A. Ochoa [a,*], A. Fries [b,c], D. Mejía [d], J.I. Burneo [a], J.D. Ruíz-Sinoga [e], A. Cerdà [f]

[a] *Departamento de Ciencias Agropecuarias y Alimentos, Universidad Técnica Particular de Loja, Campus San Cayetano, 1101608 Loja, Ecuador*
[b] *Departamento de Geología y Minas e Ingeniería Civil (DGMIC), Universidad Técnica Particular de Loja, San Cayetano Alto s/n, 1101608 Loja, Ecuador*
[c] *LCRS, Department of Geography, Faculty of Geography (FOG), University of Marburg, Deutschhausstr. 10, 35032 Marburg, Germany*
[d] *INAMHI – Instituto Nacional de Meteorología e Hidrología, 170507 Quito, Ecuador*
[e] *Physical Geography Department, University of Málaga, Campus de Teatinos, 29071 Málaga, Spain*
[f] *SEDER (Soil Erosion and Degradation Research Group), Dept. of Geography, University of València, Blasco Ibáñez, 28, Valencia 46010, Spain*

A R T I C L E   I N F O

A B S T R A C T

Understanding soil erosion processes in the Ecuadorian Andes with a tropical wet-dry climate and a variable topography, is fundamental for research on agriculture sustainable, environmental management, as well as for a stable water supply for the local populations. This work proposes method to estimate soil erosion risk in the semiarid Catamayo basin with limited data. The results show that the rainfall distribution and the erosivity along with the rugged topography, followed by the land cover (*C*-factor), are the most important factors to estimate soil erosion risk. The soil erodibility is the most important factor in the dry season for agricultural areas and where the ground cover is sparse. Soil erosion risk is higher in the centre and southwest than in the northeast of Catamayo basin. In protected areas with evergreen vegetation, the soil erosion risk is very low, even with steep slopes and high annual rainfall amounts. The methodology developed allows understanding of the soil erosion processes and the factors that lead to the spatio-temporal variability of soil erosion risk, and as a consequence improves the potential to achieve sustainability of this ecosystem through proposed conservation measures.

© 2016 Elsevier B.V. All rights reserved.

1. Introduction

The soil is a non-renewable resource (Zhao et al., 2013) that controls the biological, hydrological and geochemical cycles in the Earth System and provides the human societies with goods, services and resources (Berendse et al., 2015). There is a need to improve the land use practices to obtain a sustainable management and reduce soil erosion risk. Therefore, it is indispensable to understand how climate, topography and land cover affect the soil erosion processes and the mechanism involved (Gabarrón-Galeote et al., 2013; Lieskovský and Kenderessy, 2014). Soil is principally degraded by water erosion threatening its sustainability and causing high losses of fertile soil, which is especially pronounced in areas that are subject to inappropriate agricultural management, land abandonment, intense road construction or wild fires (Cerdà et al., 2010; Palacio et al., 2014; Panagos et al., 2014).

Soil erosion by water is also the major environmental problem for agriculture in Ecuador (Ochoa-Cueva et al., 2015), especially in the southern and southwestern parts of the province of Loja, bordering Peru. The zone has unique environmental conditions, including rugged topography, which leads to strong changes in climate within short distances, amplifying soil erosion risk (Pineda et al., 2013). The El Niño Southern Oscillation (ENSO) phenomenon plays an important role in this area, because the high rainfall intensities during ENSO events cause higher soil erosion (Tote et al., 2011).

Furthermore, land use change in this area enhances soil erosion vulnerability (Castro et al., 2013). The expansion of agriculture has put pressure on natural ecosystems not only in this region, but also in the whole country. In Ecuador, the area cultivated with maize has increased about 20% since the 1990s (FAO, 2010a). Also, investments were expanded to US$ 20.3 million during the period 2007–2009 (MAGAP, 2011), due to local and global demand of maize to produce ethanol and livestock feed. The primary natural forest was mainly converted to secondary forest or replaced by irrigated crops and dry agriculture. This change to the natural ground cover continues mainly through slash and burn activities (Bahr et al., 2013; Espinosa et al., 2012; Winckell et al., 1997a).

Ecuador has the lowest percentage of natural forest of all countries in South America (FAO, 2010b). In the study area, the ecosystem most threatened by deforestation is the Tropical Dry Forest. Deforestation has economic significance for firewood collection, construction and even for charcoal. Because of the high demand for timber, farmers prefer to exploit their lands for quick profits instead of long-term use of the forest (Castro et al., 2013).

Morgan (2005) shows an additional complication for these environments, which is caused by the need for water conservation and its

* Corresponding author.
E-mail address: paochoa@utpl.edu.ec (P.A. Ochoa).

ecological sensitivity. The change of the natural cover to pasture or crops, produces a rapid decline in organic matter content of the soil leading to a depletion and desertification risk.

In this context, our study area is the Catamayo basin in southern Ecuador, which is representative of the susceptibility of the region to land degradation because of the various climatic, topographic and land cover characteristics that lead to high soil erosion risk. However, understanding soil erosion process in this region is hampered by the scarcity of data on erosivity, erodibility and the traditional form of managing the soil resource (Ochoa et al., 2014; Romero et al., 2007; Tote et al., 2011), which is similar to many parts of the world (Cerdà, 1998, 2000; Chavez, 2006; Ruiz-Sinoga and Romero, 2010).

There are various empirical soil erosion models, such as the Revised Universal Soil Loss Equation (RUSLE) (Renard et al., 1997), Soil Loss Estimation Model for Southern Africa (SLEMSA) (Stocking, 1981), and the European Soil Erosion Model (EuroSEM) (Morgan et al., 1998); which facilitate the calculation of soil erosion risk at different locations. However, to apply these models outside their area of origin and validation, local climatic and soil data is required as an additional input. For this reason, there is increasing interest to develop methodologies adapted to local conditions, identifying areas and quantifying soil erosion risk to propose sustainable management practices (Nigel and Rughooputh, 2010a; Zhao et al., 2013). The use of stochastic models to estimate rainfall erosivity for areas with limited data (i.e. generate synthetic data series from simple statistical characteristics of existing data) can be a useful tool to generate sequences of the necessary input data for empirical models (Morgan, 2005). Geographic Information Systems (GIS) can display the digital input data on cartographic maps and help to calculate, understand and explain the soil erosion risk for the required areas on the Earth's surface.

This work attempts to provide the necessary seasonal details for estimation of soil erosion risk at regional scales, providing a methodology for policy-makers and managers to validate and approve their taken decisions. The study, executed in the semiarid Catamayo basin, seeks to advance the understanding of soil erosion risk under strong anthropogenic pressure in the Ecuadorian Andes, examining (i) the influence of altitude and topography on the climatic factors of rainfall and air temperature; (ii) soil erosion risk during the dry and the wet season; and (iii) the most important factors controlling soil erosion vulnerability in this semiarid basin.

2. Study area

The Catamayo watershed is located between 3°39′S and 4°31′S (latitude), 79°05′W and 80°11′W (longitude) in the south of Ecuador, province of Loja, close to the border with Peru (Fig. 1). The Catamayo River has a length of 120 km, whose watershed covers an area of 4184 km^2. This river is one of main tributaries of the Ecuadorian–Peruvian hydrographic system (17000 km^2), called the Catamayo–Chira Basin, which drains into the Pacific Ocean (Tote et al., 2011). The Catamayo River supplies potable water for the people in southern Ecuador and northern Peru and also for the irrigation systems inside the basin. The average annual water flow is 35 m^3/s, which significantly decreases during the dry season (22 m^3/s; Oñate-Valdivieso and Bosque, 2010).

In comparison to the northern Andes of Ecuador, which are characterized by two distinct mountain ridges (Eastern and Western Cordillera), the Southern Highlands do not show this strict separation of the cordilleras. The Eastern Cordillera reaches altitudes up to 3900 m a.s.l. near the Peruvian border, whereas the Western Cordillera only rises up to 2500 m a.s.l. (Winckell et al., 1997b). The lower altitudes of the Western Cordillera facilitate the interaction with the Ecuadorian coast. The Catamayo Basin has a strong altitudinal gradient, reaching from 240 m a.s.l. in the southwest to 3760 m a.s.l. in the northeast (Fig. 1a).

The study area is characterized by an alternation between valleys and ridges within short distances, which leads to different climate conditions due to the fast changing topography (complex terrain; Fig. 1b).

The air temperature mainly depends on the altitude (Richter et al., 2009), whereas the rainfall depends on wind speed and direction, which is modified by the topographic conditions, forming barriers and pathways for humidity transport (Fries et al., 2014). The rainy season is during austral summer (December to May), when the tropical easterlies are frequently interrupted by low westerlies, carrying moisture from the Pacific Ocean up to the study catchment (Pineda et al., 2013). In the dry season (June to November) the tropical easterlies prevail, bringing dry and sunny weather to the study area, because the higher Eastern Cordillera forms a barrier, blocking the humidity transport from the Amazon Basin.

The tropical dry forest grows in the vicinity of the Ecuadorian coast, due to the annual precipitation distribution (dry period >6 months), evincing one of the most conspicuous features of this forest type: seasonal loss of the tree leaves (Maass and Burgos, 2011). Due to the influence of the south Pacific Anticyclone during most of the year, the vegetation is characterized by semiarid species (spare brushy vegetation), especially at the valley bottom and at the western part of the study area, where altitudes are lower and air temperature higher. Around 60% of the Province of Loja is covered by deciduous and semi-deciduous dry forests (Aguirre and Kvist, 2005). The maize production with conventional tillage is the dominant crop during the wet season (Castro et al., 2013), whereas sugarcane grows in secondary valleys (e.g. Malacatos, Vilcabamba) during the whole year using irrigation systems. Due to the general wind direction from the east (Amazon Basin - tropical easterlies) the annual precipitation is highest at the upper eastern mountain ridge, where air temperature is lower and tropical humid forest and the páramo are formed (Richter et al., 2009).

3. Material and methods

Three landforms or zones were established in the basin using the ArcGIS 9.2 software and its classification tool called Natural Breaks. This tool identifies break points by picking the class breaks those best group similar values and maximizes the differences between classes. Our watershed was classified using as input data altitude and slope derived from a digital elevation model (DEM), as well as an air temperature map (Fig. 4) with a resolution of 100 m × 100 m.

The first zone corresponds to the lower area called Dry-Farming and Irrigation Zone (DFIZ) from 240 to 1400 m a.s.l., with a mean annual temperature over 21 °C. This zone generally shows slight slopes varying from 0 to 16%. The middle area, called Dry-Farming Southern Highlands (DFSH) reaches from 1400 to 2200 m a.s.l. and has a mean annual temperature between 15.5 and 21 °C. The topography is characterized by steeper slopes from 16 to 30%. The areas above 2200 m a.s.l. are mainly located in the eastern part of the basin, called Wet-Land Southern Highlands (WLSH), which are characterized by extreme slopes between 30 and 58% and a mean annual air temperature below 15.5 °C. Fig. 1a, shows the three classified zones.

These three zones are consistent with the major morphopedological sets of the Southern Highlands of Ecuador proposed by Winckell et al. (1997b); the wet rocks masses in WLSH, the slopes of transition in DFSH and depressed areas with severe drought in DFIZ.

3.1. Rainfall erosivity

The climatic data for the study was provided by a network of 24 rain gauges operated by the Ecuadorian Weather Service (INAMHI), and 2 automatic meteorological stations from Thiess — Clima (Germany), situated at the eastern edge of the watershed (TIRSTA and PARSTA, see Table 1). For this study, data from 1990 to 2013 was used and quality controlled by INAMHI. Compared to other Ecuadorian basins the rain gauge density is higher 1.7 per 174 km^2 (Ochoa et al., 2014) in the Catamayo catchment and only few missing or erroneous data were found.
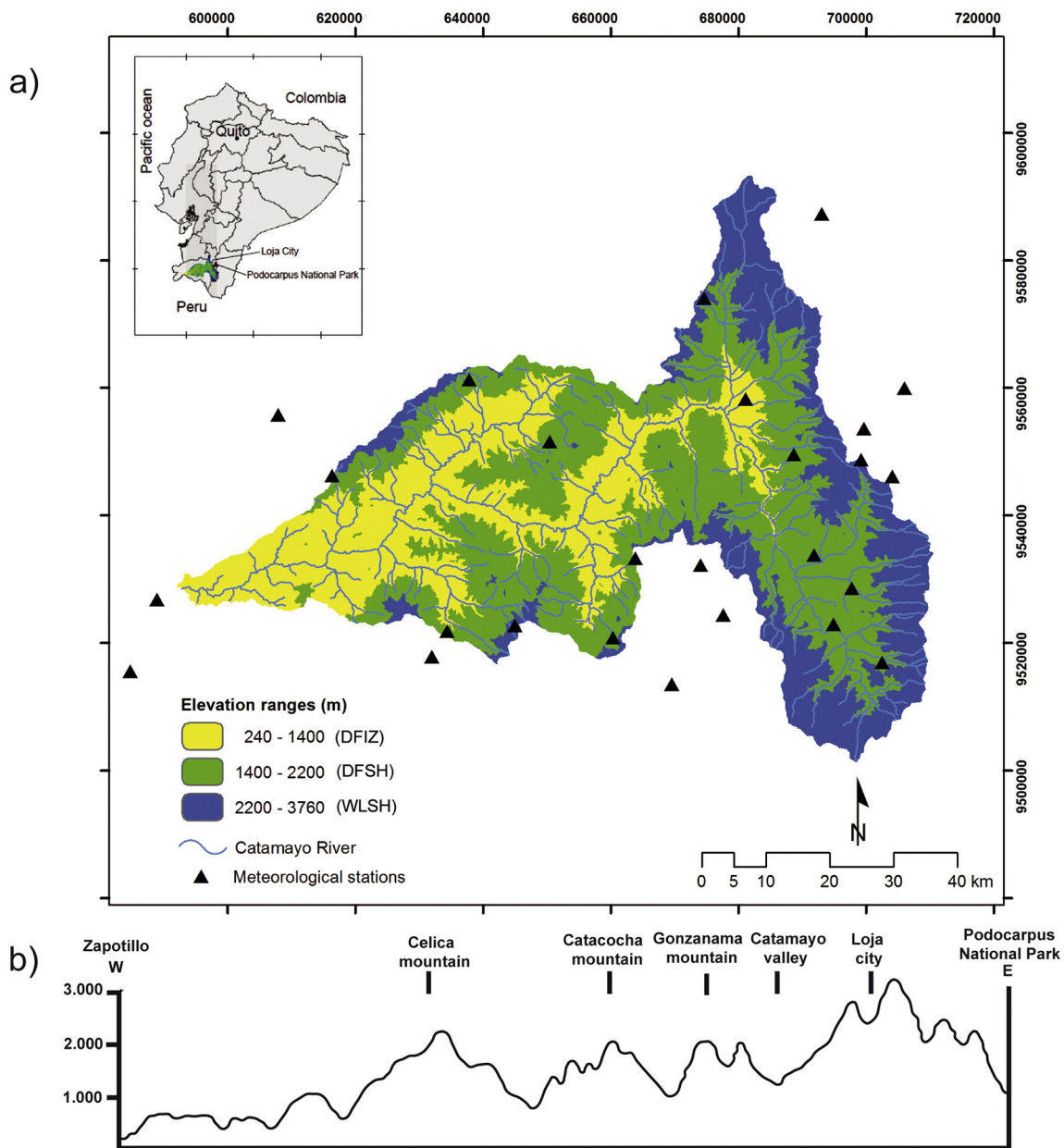
Fig. 1. Location of the Catamayo basin (a) natural breaks (elevation ranges), (b) altitudinal gradient of the Southern Highlands of Ecuador.

However, the climatological records (average monthly precipitation PCP — air temperature TEMP) were analyzed with the "Climatol" R statistical package that contributes to the homogenization of climatic series (Guijarro, 2011). Thereby, outliers and errors in the data set were detected and not included in the study. After this, the gaps in the data series are filled by a homogeneity analysis using the Standard Normal Homogeneity Test (SNHT) proposed by Alexandersson (1986). The SNHT is a statistical model that uses an orthogonal regression type II, which determines the range of the normalized data of a variable (V) with its mean and standard deviation. Finally, to check the consistence and homogeneity of information data of TEMP and PCP a double mass analysis was used. This analysis determines if there is a need for corrections of data, considering the changes in data collection procedures or other local conditions. Such changes may result from a variety of things including changes in instrumentation, changes in observation procedures, or changes in gauge location or surrounding conditions. The estimation of monthly accumulated volume of each station over a period of 23 yr of data was used to apply this analysis. In this analysis the

parameters considered were: (i) comparison of data accumulated between neighboring stations, (ii) similar altitude range and (iii) exposure to the same meso/synoptic climatological feature (e.g. El Niño-Southern Oscillation — ENSO). From the resulting 23-year data set, the PCP and TEMP were calculated.

To regionalize the average monthly precipitation, ordinary kriging was applied as Cedeño and Cornejo (2008) recommend for the spatial interpolation of rainfall data over complex terrains. Kriging is a method of interpolation based on statistical models that can predict unknown values from data observed at known locations. The air temperature was interpolated using kriging with detrended raw data, because the temperature depends directly on the altitude (Fries et al., 2009, 2012).

The erosivity (R-factor) was calculated using the equation proposed by Renard and Freimund (1994), because the R-factor equation of Renard et al. (1997) needs rainfall intensity, which is not available for the study area. Furthermore, the Modified Fournier Index (MFI) was integrated into the equation as Renard and Freimund (1994) recommended (see Eq. (1)). The R-factor is a good local parameter of erosivity

Table 1
General conditions of weather stations near the study area (based on 23-years average).

No.	Weather station	Lat. S	Long. W	Altitude [m a.s.l.]	Average rainfall [mm yr^{-1}]	Average annual temperature [°C]
1	Alamor	4° 01′	80° 01′	1250	1301	*
2	Cajanuma	4° 04′	79° 12′	2267	1212	*
3	Cariamanga	4° 20′	79° 33′	1950	1149	17.9
4	Catacocha	4° 03′	79° 38′	1808	862	*
5	Catamayo-(airport)	3° 59′	79° 22′	1250	397	24.2
6	Celica	4° 06′	79° 57′	1904	1017	15.6
7	Colaisaca	4° 19′	79° 41′	2410	1029	*
8	Changaimina	4° 13′	79° 31′	1935	1160	*
9	Gonzanamá	4° 13′	79° 25′	2042	1129	16.9
10	La Argelia	4° 02′	79° 12′	2160	998	16.2
11	Lauro Guerrero	3° 58′	79° 45′	1910	986	*
12	El Cisne	3° 51′	79° 25′	2218	1157	*
13	El Lucero	4° 23′	79° 28′	1180	847	*
14	El Tambo	4° 04′	79° 18′	1580	819	*
15	Malacatos	4° 12′	79° 16′	1453	668	20.0
16	PARSTA	4° 06′	79° 09′	3410	2429	6.8
17	Quilanga	4° 18′	79° 23′	1819	1144	*
18	Quinara	4° 18′	79° 14′	1559	854	20.8
19	Sabiango	4° 21′	79° 48′	734	856	*
20	San Lucas	3° 43′	79° 15′	2525	1093	*
21	Saucillo	4° 16′	80° 11′	328	618	*
22	Sozoranga	4° 19′	79° 47′	1427	1134	*
23	TIRSTA	3° 58′	79° 08′	2814	1464	9.9
24	Vilcabamba	4° 15′	79° 13′	1563	944	21.0
25	Yangana	4° 22′	79° 10′	1835	1126	19.1
26	Zapotillo	4° 22′	80° 14′	223	532	25.8

* Rain gauge only.

widely used in the tropics (Nigel and Rughooputh, 2010b; Vrieling et al., 2014).

$$R_{(x,y)} = 95.77 - 6.081\ F + 0.4770\ F^2 \qquad (1)$$

where $R_{(x,y)}$ is the R-factor in (MJ mm ha^{-1} h^{-1} yr^{-1}) at grid cell (x,y) and F is the MFI.

The modified Fournier's index is expressed according to Arnoldus (1977):

$$F = \frac{\sum_{i=1}^{12} pi^2}{P} \qquad (2)$$

where p_i is average monthly precipitation and P average annual precipitation.

To demonstrate the seasonal climate influence on soil erosion risk inside the watersheds the months of March (wettest month = rainy season) and August (driest month = dry season) were selected. EI_{30} was predicted using the average monthly precipitation as Chavez (2006) proposed. The coefficient of determination (R^2) of this regression equation is 0.802 (Eq. (3)):

$$EI_{30} = 3.88p - 37.23 \qquad (3)$$

where p is the monthly precipitation.

3.2. Soil erodibility

The soils samples were taken along an altitudinal climo-sequence that crosses seven districts of the province of Loja in the Catamayo watershed. The sampling sites were selected under the condition to cover as many areas of different landforms, climate and altitude as possible. The sampling altitudes range from 240 m to about 2400 m a.s.l., including areas of tropical dry forest, agriculture and pasture. The areas of tropical humid forests could not be sampled efficiently because the majority of this land cover is declared nature reserve (Fig. 2). The sampling sites were geo-referenced using Garmin GPS (accuracy 3 m).

According to the objectives of this study, the first mineral horizon of the soil profile (top-soil) was analyzed, because only this layer is directly affected by rainfall and runoff. However, also the B horizon was sampled for future studies, analyzing the nutrient availability inside the soils. The horizons were described separately by depth, assessment of texture and structure according to the FAO guidelines (2006). The whole sampling process was photographically recorded, taking pictures of the landscape and the soil profile. The permeability of each soil sampling site was estimated qualitatively in the field through hydraulic conductivity using a disk infiltrometer with the method proposed by Zhang (1997).

The soil sampling was part of another project, called "Generation of geo-information for land management nationwide" executed by the CLIRSEN (Centro de Levantamientos Integrados de Recursos Naturales por Sensores Remotos) and by the National Secretariat of Planning and Development of Ecuador (SENPLADES). The samples were taken and methodologically analyzed by the Universidad Técnica Particular de Loja (UTPL) and compared to the official information provided by the National Information System (SNI) of the Ecuadorian Government available online (http://sni.gob.ec/web/inicio/planes-de-desarrollo-y-ordenamiento-territorial). A set of 321 soil samples were used to estimate the soil erodibility in the Catamayo basin (Fig. 7).

In the laboratory, the soil samples were air dried and sieved through a 2 mm mesh size. The soil particle size distribution was determined using the hydrometer method (Bouyoucos, 1962). The proportion of very fine sand was obtained by wet sieving. The soil organic matter (OM) was determined by humid oxidation using the Walkley–Black method (Soil Survey Staff, 1996). For more information about the laboratory analyzes, please refer to Ochoa-Cueva et al. (2015).

The soil erodibility (K-factor) was calculated according to Renard et al. (1997) and converted into SI units of t ha h ha^{-1} MJ^{-1} mm^{-1}, as follows:

$$K = 0.277 * 10^{-6}\ M^{1.14}(12 - OM) + 0.0043\ (s - 2) + 0.0033(p - 3) \qquad (4)$$

where K is the erodibility rate, M is (% silt + % very fine sand) $* (100 - %$ clay), OM is organic matter (%), s is the soil structural class ($s = 1$: very fine granular, $s = 2$: fine granular, $s = 3$, medium or coarse granular,
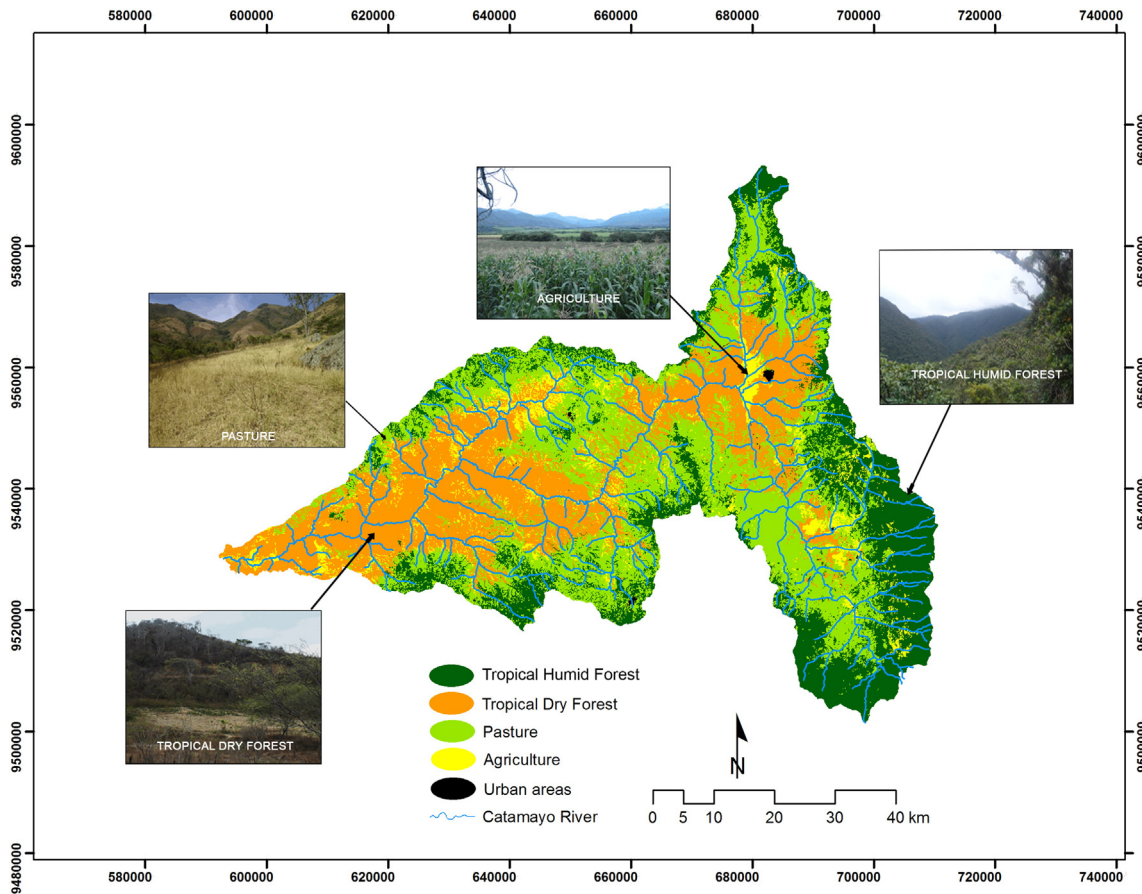
Fig. 2. Land cover map of the Catamayo basin.

$s = 4$: blocky, platy or massive); determined on the first horizon of the soil profile according to the guidelines of FAO (2006), and p is a permeability class ($p = 1$: very rapid, $p = 2$: mod. to rapid, $p = 3$: moderate, $p = 4$: slow to mod., $p = 5$: slow, $p = 6$: very slow).

The K-factor layer was then calculated based on Eq. (4) for each soil sample point and the results interpolated in a GIS using ordinary kriging method. Pérez-Rodríguez et al. (2007) suggested derivation of soil erodibility from geologic or physiographic data using kriging. However, the geologic maps are not available for the basin at a similar scale to our generated cartographic maps. In this work were used the soil erodibility, altitude and slope (DEM) to estimate a reliable distribution from the dispersed sample points.

3.3. Topographic factor

A 100 m DEM of the study area was downloaded from Institut de Recherche pour le Développement in Ecuador. This DEM was used to parameterize the topographic factor (Nigel and Rughooputh, 2010a). This resolution selected depicts most of the agricultural production units (UPAs in Spanish) used in the province of Loja (one hectare upwards), according to the latest National Census for Agriculture and Livestock (http://sinagap.agricultura.gob.ec/censo-nacional-agropecuario) as well as to Bahr et al. (2013). According to FAO (2006), Nigel and Rughooputh (2010b) and field experience, the topographic factor of slopes inside the basin was classified into five levels of erosion risk: 0–5% (very low), 5–10% (low), 10–20% (moderate), 20–40% (high) and >40% (very high). In terms of topographic factors the watershed was divided into 3% very low, 6% low, 16% moderate, 41% high and 33% very high erosion risk areas.

3.4. Land cover factor

The land cover factor (C-factor) was defined from the official vegetation map and land use map of the province of Loja with a resolution of 1:25,000 (Cueva and Chalán, 2010). This land cover map has 29 typologies, including clouds and shadows. The map was developed from ASTER satellite images acquired by the Provincial Government of Loja (http://glovis.usgs.gov) and accuracy and quality checked by the Agency of Geographic Information and Remote Sensing of Ecuador — CLIRSEN. However, Oñate-Valdivieso and Bosque (2010) grouped the detailed regional land cover classification map of the Catamayo-Chira basin in only five main classes: Evergreen-Tropical Humid Forest (THF), Tropical Dry Forest (TDF), Pasture, Agriculture, and other uses (urban areas and rivers), which were also used to calculate the soil erosion sensitivity maps in this study (Fig. 2). The ground covers for TDF, pasture (seasonal grass) and agriculture were adapted to their seasonal variation using the specific monthly values, as it can be verified in Table 2. These specific values of the C-factor were taken from the RUSLE guide (Morgan, 2005), and the monthly variability was estimated by the degree of soil protection and the seasonal leaves and plant growth (0, 25, 50 and >75%). The first abundant rainfall starts in December (Fig. 3) initiating the annual plant growth. The influence of ground cover on the soil erosion risk was illustrated for the driest and wettest month as well as for the average annual.

4. Results

The outputs of the methodology implemented in the Catamayo watershed (an area of 4184 km^2) comprise a set of maps with a 100 m cell size.

Table 2
Averages monthly and annual of values of the C-factor according to the land cover types.

Land cover types	Description	Average monthly and annual of values of the C-Factor												
		Dec	Jan	Feb	Mar	Apr	May	Jun	Jul	Aug	Sep	Oct	Nov	Year
Tropical humid forest	This forest type should not be considered primary forest because it has already had some intervention. The C-factor value is constant (0.003) because this forest maintains its coverage all year (very low erosion risk).	0.003	0.003	0.003	0.003	0.003	0.003	0.003	0.003	0.003	0.003	0.003	0.003	0.003
Tropical dry forest	Includes deciduous and semi-deciduous forest that growing in tropical areas subject to severe climatic seasonality. Higher values correspond to the months that TDF lacks leaves; and with the first rains leaf regeneration reactive.	0.1	0.025	0.01	0.01	0.01	0.025	0.05	0.1	0.1	0.1	0.1	0.1	0.061
Pasture	In the seasonal pastures, the higher values are associated with overgrazing areas and dry season; and the opposite, lower values correspond to zones with pasture in good conditions and in rainy season.	0.1	0.05	0.01	0.01	0.01	0.01	0.05	0.1	0.1	0.1	0.1	0.1	0.062
Agriculture	The higher values correspond to the maize grown in rainy season and conventional tillage. Also, agricultural production is continuous in some areas of the basin (e.g. sugar cane all year), for this reason the values described in dry seasonal period are not lows.	0.55	0.55	0.45	0.33	0.23	0.13	0.13	0.13	0.13	0.13	0.13	0.13	0.252

4.1. Relations found between altitude, topography and climatic conditions

The average annual air temperature over a period of 23 yr is plotted in Fig. 4. The air temperature is directly proportional to the altitude and decreases with height. Fig. 5a, described a very good correlation between temperature and altitude was found for the average annual temperature ($R^2 = 0.92$). Also the air temperature has a good relationship with land cover see Figs. 2 and 4. In contrast to the air temperature the correlation between altitude and rainfall was ($R^2 = 0.58$ — Fig. 5b), which is due to the topography that forms barriers and pathways for the humid air.

The DFIZ contains semiarid areas at the outlet (Zapotillo canton 240 m a.s.l.) and arid areas at the upper eastern part (Catamayo City 1250 m a.s.l.). This discrepancy is caused by the orographic situation of Catamayo City (Fig. 1b), which is surrounded by mountain barriers, limiting the humidity transport from the west, north, east and south

(Fig. 1a), leading to 12-month of aridity. Around the city rainfall generally occurs during the austral summer months when local thunderstorms are formed. However, due to the arid conditions annual rainfall quantities are very variable with highest values around 400 mm yr^{-1} (Table 1).

The lower parts of DFIZ have semiarid conditions (10 dry months) and show slightly higher rainfall quantities (between 400 and 650 mm yr^{-1}; Table 1). This is due to the orientation of the catchment, which is open to the southwest and humidity can enter the valley from this side. In the lower western parts rainfall occurs during the austral summer months too, when the general wind direction is frequently changed to the west, carrying humid air from the Pacific Ocean up to the valley. During ENSO-events rainfall quantities are significantly higher for the whole study catchment, due to the higher sea surface temperatures of the Pacific, causing enhanced evaporation and therefore higher moisture content in the air.
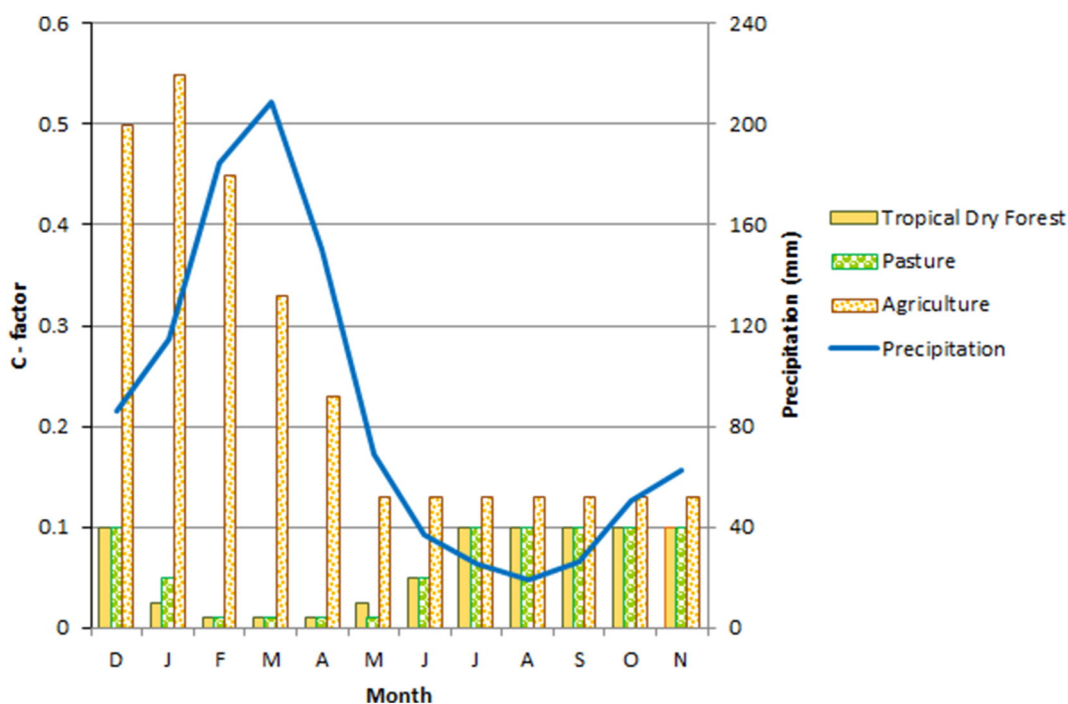

Fig. 3. Monthly trend of soil erosion risk according to seasonal changes of the C-factor.
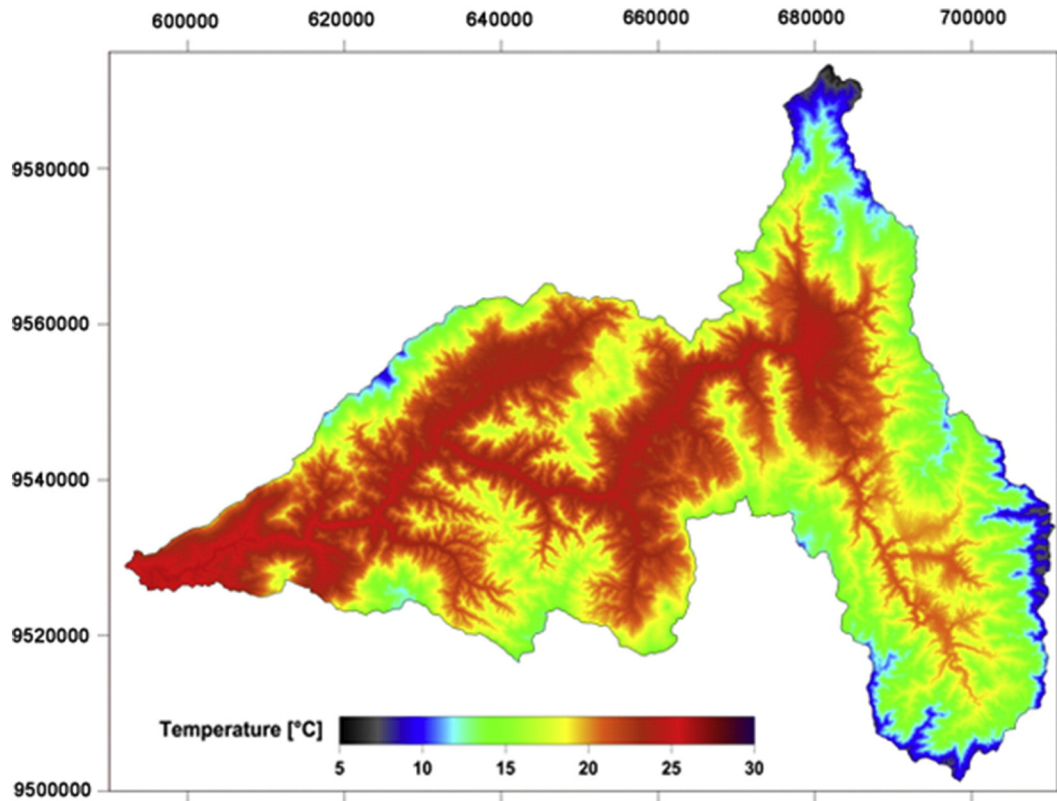
Fig. 4. Annual air temperature in the study area.

Fig. 6 depicts the spatial distribution of precipitation, the monthly EI_{30} of the extreme months and the R-factor. The orientation of the mountain ridges favor or hinder the humidity transport into the watershed. During austral summer (March; Fig. 6a) the humid air, coming from the Pacific Ocean, is forced to ascend at the western mountain ridge forming a barrier (Celica Mountain) and precipitation is enhanced on the lower windward slope reaching highest values above 300 mm month^{-1}. Highest rainfall amounts inside the study catchment are observed at the Catamayo River outlet and at the southern mountain ridge. This is caused by the orientation of the valley outlet and the structure of the western barrier, which is lower at its southern parts, wherefore a higher content of moisture can pass the barrier, leading to higher rainfall amounts for this part of the valley. During austral winter (August; Fig. 6c) a severe drought is observed inside the study catchment,

because wind comes from the east and humidity transport is blocked by the highest mountains of the eastern ridge (Podocarpus National Park). The eastern barrier hampers humidity transport inside the watershed; only the highest parts at the eastern barrier still receive small monthly rainfall amounts, which quickly decrease after the barrier further to the west. Highest rainfall amounts during the dry season are recorded from the Yangana station with values slightly above 90 mm month^{-1} (data not shown).

The average yearly rainfall (Fig. 6e) closely follows the distribution observed during March (Fig. 6a), but with significant higher values. In contrast to March, the annual map shows highest rainfall amounts at the upper eastern ridge inside the catchment (values up to 1100 mm yr^{-1}). This is due to the general wind direction from the east, carrying the moisture from the Amazon Basin up to the eastern
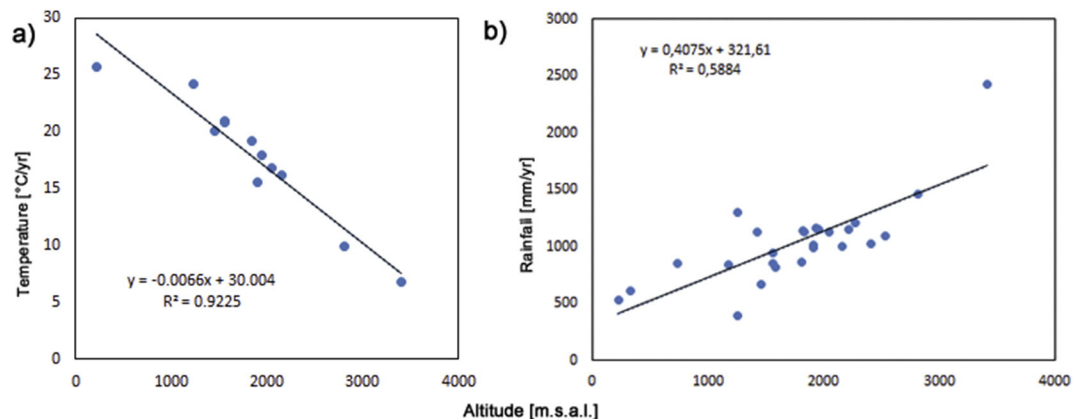

Fig. 5. Annual correlations between (a) air temperature and altitude, (b) rainfall and altitude.
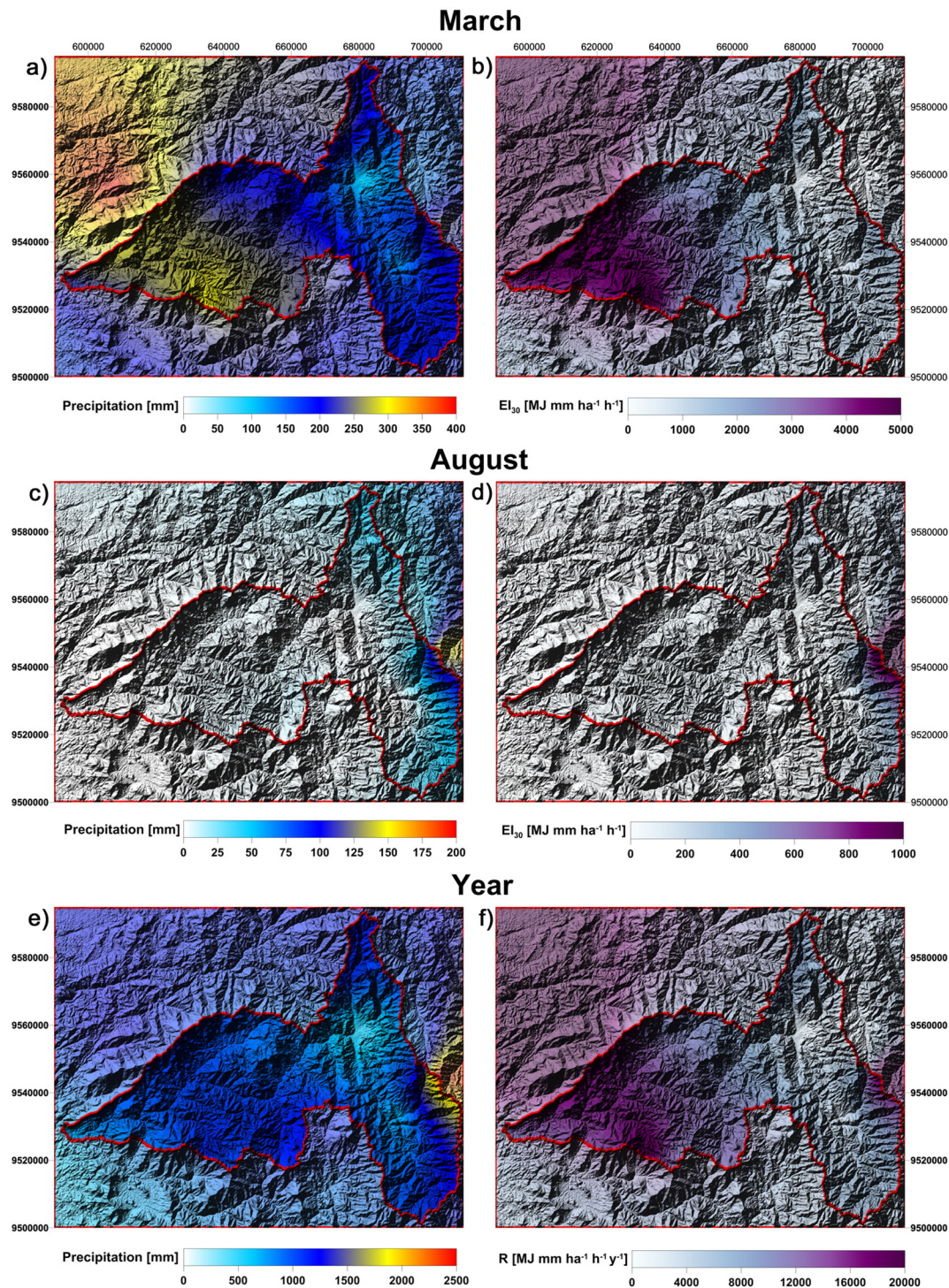
Fig. 6. (Left column) Spatial distribution of rainfall in mm a, c, e. (Right column) Ei_{30}, for (b) March, (d) August, and erosivity (f) annual map (MJ mm ha^{-1} h^{-1} yr^{-1}).

mountain ridge. The strong barrier effect of this mountain chain hampers the humidity transport inside the watershed; only the highest parts receive frequent precipitation.

4.2. Soil erosion risk processes

Fig. 6 (right column) shows the influence of the weather conditions on the processes of soil erosion risk. The EI_{30} values ranged from 256 to 5022 MJ mm ha^{-1} h^{-1} for the wettest month (March). The lowest values are shown around the Catamayo City and the highest values are calculated for the western parts. For the driest month (August)

EI_{30} values ranged from 0 to 521 MJ mm ha^{-1} h^{-1}. In this month values are generally low for the entire basin, and only at the upper eastern ridge do the values increase (eastern barrier). The average annual value of the R-factor for the whole basin was found to be 10,249 MJ mm ha^{-1} h^{-1} yr^{-1}.

The soil erosion susceptibility map with the decision rule is shown in Fig. 7. About 0.6% of the total catchment area is classified as very low, 11.5% low, 30.8% moderate, 56.1% high and 1% very high. The main part of the basin shows moderate to high soil erosion susceptibility.

The land cover map with the main classes (THF, TDF, Pasture and Agriculture); shows a good relation with the landforms and the climate.
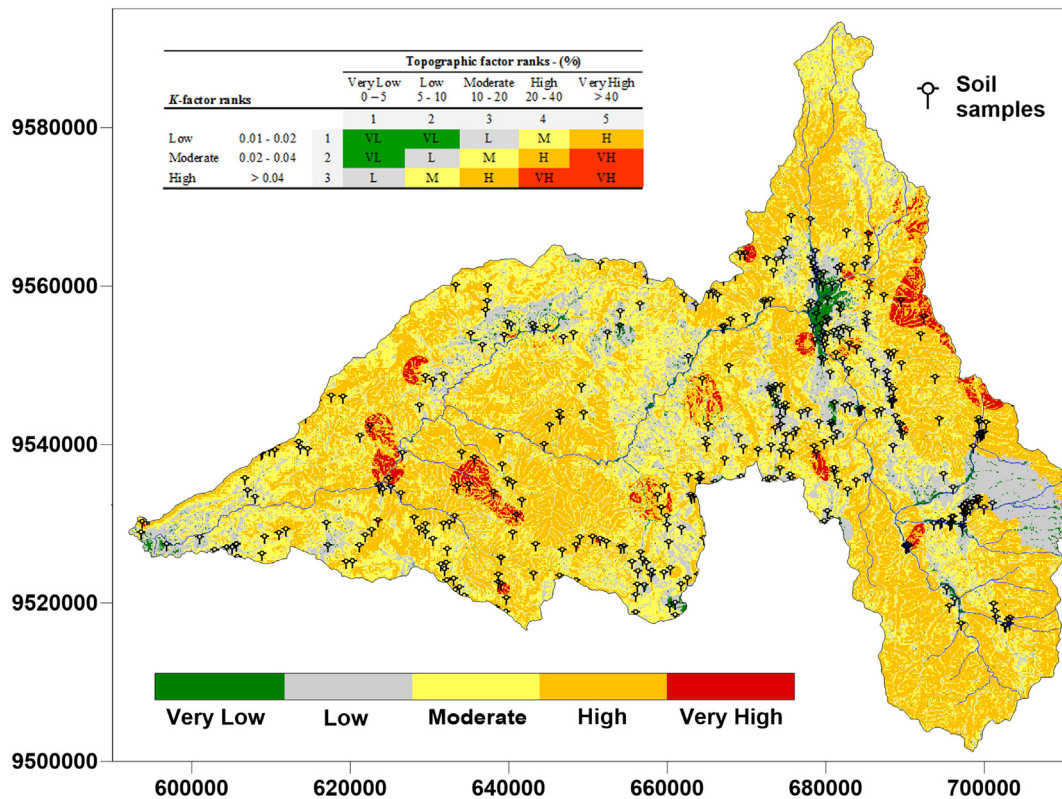
Fig. 7. Soil erosion susceptibility map (*K*-factor + topographic factor); with decision rule.

The changes of the vegetation are mainly caused by the climate conditions and by the anthropic management for the agriculture land. The THF covers about 24.3% of the catchment area and is located in the upper parts (WLSH) of the watershed, where humidity is also higher. This coverage maintains its canopy all year round, providing very good soil protection during any season. The TDF takes about 31.1% of the total surface and is mainly present in the lower parts of the basin (DFIZ). This vegetation type is similar to savannah. The TDF is dominantly used for uncontrolled grazing of cows and goats and also for timber production. About 36.5% of the study area is pasture, which is mostly uncultivated land, used for grazing. The pasture (*Panicum maximum*) grows naturally along the western Andes mainly where humidity is high. The cultivated pastures, like *Pennisetum clandestinum*, are located in small areas at higher elevations, where water availability is sufficient for irrigation. The ground covers in this specific class vary from herbaceous to brushy vegetation. This fact makes it difficult to harmonize the information of other studies in the region, because there is no common definition for the land use class "Pasture". Agriculture (dry-farming) is present at all altitudinal ranges, covering about 7.6% of the

basin. Maize is the predominant crop for this farming system with conventional tillage, a technique prevalent throughout the study area. In the cities of Zapotillo and Catamayo the agriculture changes abruptly to intensive irrigation systems. The main crops are maize and sugar cane respectively. The urban areas and rivers take about 0.5% of the basin area and were set to 0, which means there is no erosion risk. In summary, pasture and TDF are the predominant land covers, which together account about 70% of the total area of the basin (Fig. 2).

In Fig. 8 the soil erosion sensitivity maps (susceptibility + *C*-factor maps in relation to the seasonal and annual climatic conditions) are shown. Our results are consistent with other studies such as Bakker et al. (2008) and Panagos et al. (2015), which have modeled *C*-factor. The degree of soil protection in TDF, pastures and agriculture is low, mainly during the dry season (June to November), due to the lack of canopy (Fig. 8b). However, some species of the TDF as the Guayacán (*Tabebuia chrysantha* or *Tabebuia billbergii*) and the *Ceiba trichistandra* begin the process of defoliation approx. 2 months before the start of the dry season, but there are also species that do not completely defoliate during the same period (*Cynophalla mollis* and *Acacia macracantha*).
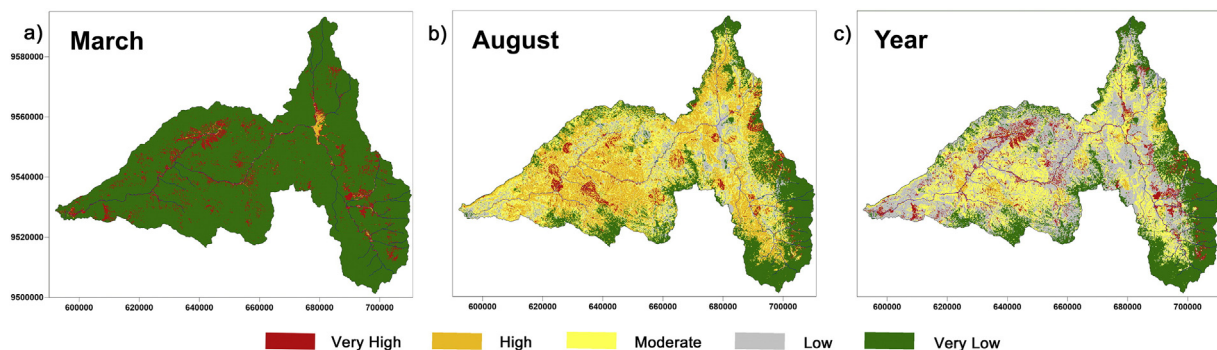

Fig. 8. Soil erosion sensitivity maps (Susceptibility map + *C*–factor maps) for; (a) March, (b) August, and (c) average annual.

The assigned values for the agricultural use remain constant during the dry season, due to the ongoing irrigation management for some valleys and areas near to rivers, these zones is best viewed in Fig. 8a.

In the Catamayo Basin, a close relationship between the (K-factor and slope), land cover (C-factor) and erosivity (R-factor) exists; e.g. the ground cover depends on the climatic factors such as rainfall and air temperature (Figs. 2 and 4); but also it depends of the soil conditions (texture, OM, structure, permeability and topography). Agricultural activities are not possible on steep slopes. The final cartographic product (Fig. 9) shows the soil erosion risk maps at seasonal and annual timing, with these relationships between erosivity, erodibility, topography and land cover. According to the climatic seasonality March is the month with the highest risk of soil erosion in scattered areas throughout the basin and the highest values in crops areas (Fig. 9a). By August, due to low rainfall is lowest soil erosion risk; the highest values are in pasture areas and near to the Eastern cordillera (see Fig. 9b).

5. Discussion

This cartographic study described the spatio-temporal variability of soil erosion risk on a regional scale. It clearly shows the critical months, hotspots and land uses which are more susceptible to erosion. A close relationship between climate, altitude and topography could be shown for the Catamayo watershed. The mean monthly air temperature does not vary significantly during the year, and shows a good correlation with altitude and land cover (Fries et al., 2009) In this context the air temperature could be a factor to consider in studies of soil erosion to evaluate the impact of land management practices in rural areas sensitive to desertification (Kairis et al., 2015).

The relationship between precipitation–altitude cannot be assumed for regional studies in mountain areas, due to the influence of the landforms, forming barriers and pathways. However, local studies show that the altitudinal gradient of precipitation can be applied for small watersheds, located within the same mountain ridge and having the same exposure (e.g. Ochoa-Cueva et al., 2015). The windward/leeward orographic effects caused by the topography are difficult to detect and can be analyzed using remote sensing (Ochoa et al., 2014). Pineda et al. (2013) describes that the western Andes cordillera and the shape of its branches have an imposing effect on the rainfall distribution. In the study area the rainfall distribution, and therefore the annual R-factor, does not depend directly on the altitude; more important is the location respective to specific mountain barriers and pathways for the humidity transport. It can be verified in Figs. 1b and 6.

During the dry season (Jun. Jul. Aug.–Sep. Oct. Nov.) the influence of sea surface temperature anomalies is weak (Jun. Jul. Aug.) or rather insignificant (Sep. Oct. Nov.) Pineda et al. (2013). The humidity comes from the Amazon Basin during this season, because the general wind direction is from the east (Richter et al., 2009). The high eastern mountain ridge in the east hampers the humidity transport into the valley. Consequently, the growth of the vegetation and agricultural activities are

limited during this time period (Aguirre and Kvist, 2005; Maass and Burgos, 2011; Castro et al., 2013). The strong contrasts between the dry and rainy seasons, the insufficient ground cover, the sandy formations without consistency and the steep slopes generated the morphodynamic conditions in the study area (see Figs. 8 and 9).

The annual soil erosion risk map (Fig. 9c) shows that 17.9% (749 km^2 of the Catamayo basin) can be classified with very high erosion risk. The areas with high and moderate erosion risk cover 21.3% of the area. The western parts as well as the area of the river outlet have the highest risk of erosion. The mountain ridges do not show such high values, because these parts preserved THF and only small patches are deforested. The main factors that influence the soil erosion risk in the Catamayo basin are the erosivity factor (R-factor), as found by Nigel and Rughooputh (2010a), as well as the land cover factor (C-factor). Fig. 9c makes it clear that poor land cover increases soil erosion risk; here mainly caused by runoff. Especially during the dry season the management of vegetation cover is important to reduce the volume of sediment in the rivers (García-Orenes et al., 2009; Mandal and Sharda, 2013; Kairis et al., 2015). However, the erosivity factor is low for more or less 50% of the basin (Fig. 6f); some hotspots are located in the east and the center, where precipitation is high and vegetation cover sparse.

The high soil erosion risk in the DFIZ zone is confirmed by Winckell et al. (1997b) who found evidence of colluvio-alluvials formations deposited in the river banks. The relationship between climate, topography and land cover can be seen as a key factor to understand the soil erosion in the southern highland of Ecuador.

Other studies (e.g. Cerdà et al., 2009; Ruiz-Sinoga and Romero, 2010; Zhao et al., 2013), describe the ground cover as the key factor to prevent soil erosion in semiarid mountain watersheds, too. In the Catamayo Basin the agriculture shows a division in production patterns depending on land holding at the three altitudinal zones, proposed for the first time in this work (Fig. 1). In the upper basin (WLSH), traditional minifundia or latifundia are common with mixed (citrus, banana and coffee) or rotated cultivation using the fallow system. At DFSH smallholders (family farms) operate near the subsistence level. Generally, when agricultural yields are low and the landholding is big enough, the farmers use slash and burn agriculture, otherwise they abandon the land. For this agricultural practice or way of land use, we should propose more environmental education and land conservation policies. In the lower basin (DFIZ), some commercial farms with some level of management and mechanization are established, hiring landless employees. Monoculture of sugarcane and maize is dominant and the soil fertility is low, wherefore huge amounts of fertilizer are used.

Generally, in the Catamayo Basin the economy is based on subsistence farming with great local importance (Bahr et al., 2013); only a few products are destined for the regional market, e.g. sugar cane, corn and coffee (Castro et al., 2013). However, in times of severe drought meat and milk from livestock production is more important than any cultivated crop. Against this background, regional analysis of soil management (basin-wide) should pay more attention to the
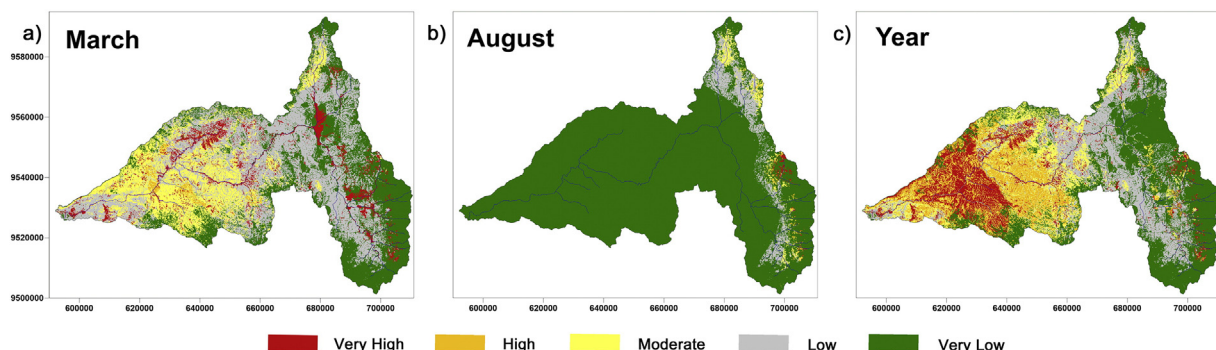

Fig. 9. Soil erosion risk maps (susceptibility map + sensitivity maps + erosivity maps) for; (a) March, (b) August, and (c) average annual.

pasture areas rather than on agriculture itself. Moreover, pasture comprises about 36.5% of the total surface of the basin, excluding the TDF (31.1%), which is also used for livestock grazing, and agriculture only occupies 7.6%.

According to some farmers and conservational activists the land use in the study area is disorganized and uncontrolled due to the intensive agriculture and overgrazing (Castro et al., 2013; Espinosa et al., 2012; Podwojewski et al., 2002). In this context, some researchers (e.g. Aguirre and Kvist, 2005; Vázquez et al., 2001) suggest to reduce or to eliminate livestock grazing in dry ecosystems. However, other studies e.g. in Savory (1999) suggest that holistic planned grazing (HPG), which means higher animal density on semiarid ecosystems but during a shorter time period, may result in higher soil-water content through the development of more ground-surface litter (Weber and Gokhale, 2011).

In order to prevent desertification processes in semiarid area of southern Ecuador, it is essential to maintain soil cover in good condition, avoiding deforestation in natural forests and maintaining soil fertility properties on active pasture sites. The natural forest and the protected areas are especially important for water sources (e.g. *Podocarpus* National Park) and favor significantly the landscape stability of the basin, too. The maintenance of existing pasture soils and their fertility depends of the adoption of new or modified soil management systems by farmers. This can be achieved with management proposals such as:

i) Adequate management of seasonal pastures and herds, e.g. using the HPG. Studies developed in the study area by Espinosa et al. (2014), describes a surprising increase in the diversity of species in plots subjected to seasonal grazing.
ii) Management of soil pastures, planting legumes that provide nutrients, therefore maintaining good levels of pasture productivity.
iii) Replace the slash and burn practices by activities more economical and ecological for land-users, such as conservation payments. A proposal on this topic is suggested by Castro et al. (2013). To avoid serious consequences of erosive rainfall due to the low vegetation cover.

Obviously, these management proposals need to be modeled and validated, as well as their appropriateness for applications for the local population in semiarid Andean regions. The soil is a complex system that needs to be studied by multidisciplinary approaches (Brevik et al., 2015; Knoke et al., 2014).

In the future, better estimates of soil erosion are possible using new technologies such as radar networks with automatic stations to analyze erosive events e.g. of ENSO and the subsequent drought to this phenomenon. Also, more research is needed at plot or UPA scales with 5–10 yr long experiments monitoring and using different models (e.g. mHM, WEPP, G2 erosion models) to determine the soil erosion risk and sediment transport more accurately, with own models or more adapted to local conditions of the Andes.

6. Conclusions

Soil erosion risk in a semiarid basin of the Andes shows a high influence of climatic seasonality and topographical conditions. During the rainy season, soil erosion vulnerability is highly influenced by the erosivity factor, followed by the *C*-factor (seasonal coverage) and to a lesser degree the topographic and soil erodibility factors. Unlike, in the dry season the soil erodibility and topographic factors become more important, influenced by the poor vegetation cover (*C*-factor).

The relationship between air temperature and altitude is consistent in this Andean basin; however, there is no obvious relationship between rainfall and altitude for regional studies due to the topographical conditions. The altitudinal gradient of precipitation can be used only for small watersheds located within the same mountain ridge and having the same exposure.

This study suggests an applicable methodology for semiarid regions with limited data to assess the spatial and seasonal patterns of soil erosion and to identify high erosion areas. This is an important input to decision makers to preserve and manage sustainably the soil and land cover in the basins.

References

Aguirre, Z., Kvist, L.P., 2005. Floristic composition and conservation status of the dry forests in Ecuador. Lyonia 8, 41–67.

Alexandersson, H., 1986. A homogeneity test applied to precipitation data. J. Climatol. 6, 661–675.

Arnoldus, H.M.J., 1977. Methodology used to determine the maximum potential average annual soil loss due to sheet and rill erosion in Morocco 34. FAO. Soils Bulletin, pp. 39–51.

Bahr, E., Hamer, U., Chamba, D., Makeschin, F., 2013. Different fertilizar types affected nitrogen and carbon cycling in eroded and colluvial soils of Southern Ecuador. Agric. Sci. 4, 19–32.

Bakker, M.M., Govers, G., Van Doorn, A., Quetier, F., Chouvardas, D., Rounsevell, M., 2008. The response of soil erosion and sediment export to land-use change in four areas of Europe: the importance of landscape pattern. Geomorphology 98, 13–226.

Berendse, F., van Ruijven, J., Jongejans, E., Keestra, S.D., 2015. Loss of plant species diversity reduces soil erosion resistance of embankments that are crucial for the safety of human societies in low-lying areas. Ecosystems 18, 881–888.

Bouyoucos, G.J., 1962. Hydrometer method improved for making particle size analysis of soils. Agron. J. 54, 464–465.

Brevik, E.C., et al., 2015. The interdisciplinary nature of soil. Soil 1, 117–129.

Castro, L.M., Calvas, B., Hildebrandt, P., Knoke, T., 2013. Avoiding the loss of shade coffee plantations: How to derive conservation payments for risk-averse land-users. Agrofor. Syst. 87, 331–347.

Cedeño, J., Cornejo, M.P., 2008. Evaluation of three precipitation products on ecuadorian coast. available at: http://wcrp.ipsl.jussieu.fr/Workshops/Reanalysis2008/Documents/Posters/P3-25_ea.pdf (Accessed 12 April 2014).

Cerdà, A., 1998. Relationship between climate and soil hydrological and erosional characteristics along climatic gradients in Mediterranean limestone areas. Geomorphology 25, 123–134.

Cerdà, A., 2000. Aggregate stability against water forces under different climates on agriculture land and scrubland in southern Bolivia. Soil Tillage Res. 36, 1–8.

Cerdà, A., Giménez-Morera, A., Bodí, M.B., 2009. Soil and water losses from new citrus orchards growing on sloped soils in the western Mediterranean basin. Earth Surf. Process. Landf. 34, 1822–1830.

Cerdà, A., Lavee, H., Romero-Díaz, A., Hooke, J., Montanarella, L., 2010. Soil erosion and degradation in Mediterranean type ecosystems. Land Degrad. Dev. 21, 71–74.

Chavez, R., 2006. Modeling soil erosion risk in Los Maribios volcanic chain, Nicaragua. Trop. Resour. Bull. 25, 50–56.

Cueva, J., Chalán, L., 2010. Cobertura Vegetal y Uso Actual del Suelo de la Provincia de Loja. Informe Técnico. Departamento de Sistemas de Información Geográfica de Naturaleza & Cultura Internacional. Gráficas Amazonas, Loja–Ecuador (http://www.naturalezaycultura.org/docs/Informe%20Cobertura%20Vegetal.pdf).

Espinosa, C.I., De La Cruz, M., Luzuriaga, A.L., Escudero, A., 2012. Bosques tropicales secos de la región Pacífico Ecuatorial: diversidad, estructura, funcionamiento e implicaciones para la conservación. Ecosistemas 21, 167–179.

Espinosa, C.I., Luzuriaga, A.L., De La Cruz, M., Escudero, A., 2014. Climate and grazing control nurse effects in an Ecuadorian dry shrubby community. J. Trop. Ecol. 30, 23–32.

FAO, 2006. Guidelines for soil description. Food and Agriculture Organization of the United Nations, Rome, p. 109.

FAO, 2010a. Statistics division. Food and Agriculture Organization of the United Nations (http://faostat.fao.org/default.aspx, Accessed 14 June 2013).

FAO, 2010b. Growing Food for Nine Billion. Food and Agriculture Organization of the United Nations (http://www.fao.org/docrep/013/am023e/am023e00.pdf, Accessed 20 June 2013).

Fries, A., et al., 2009. Thermal Structure of a Megadiverse Mountain Ecosystem in Southern Ecuador, and its Regionalization. Erdkunde 63, 321–335.

Fries, A., Rollenbeck, R., Nauß, T., Peters, T., Bendix, J., 2012. Near surface air humidity in a megadiverse Andean mountain ecosystem of southern Ecuador and its regionalization. Agric. For. Meteorol. 152, 17–30.

Fries, A., et al., 2014. Catchment precipitation processes in the San Francisco valley in southern Ecuador: combined approach using high-resolution radar images and in situ observations. Meteorog. Atmos. Phys. 126, 13–29.

Gabarrón-Galeote, M.A., Martínez-Murillo, J.F., Quesada, M.A., Ruiz-Sinoga, J.D., 2013. Seasonal changes in the soil hydrological and erosive response depending on aspect, vegetation type and soil water repellency in different Mediterranean micro environments. Solid Earth 4, 497–509.

García-Orenes, F., et al., 2009. Effects of agricultural management on surface soil properties and soil-water losses in eastern Spain. Soil Tillage Res. 106, 117–123.

Guijarro, J.A., 2011. User guide to climatol: An R package for homogenization of climatological series. R Pakages (1, 33).

Kairis, O., Karavitis, C., Salvati, L., Kounalaki, A., Kosmas, K., 2015. Exploring the impact of overgrazing on soil erosion and land degradation in a dry Mediterranean Agro-forest landscape (Crete, Greece). Arid Land Res. Manag. 29, 360–374.

Knoke, T., et al., 2014. Afforestation or intense pasturing improve the ecological and economic value of abandoned tropical farmlands. Nat. Commun. 5, 5612.

Lieskovský, J., Kenderessy, P., 2014. Modelling the effect of vegetation cover and different tillage practices on soil erosion in vineyards: A case study in vráble (Slovakia) using WATEM/SEDEM. Land Degrad. Dev. 25, 288–296.

Maass, M., Burgos, A., 2011. Water dynamics at the ecosystem level in seasonally dry tropical forests. In: Dirzo, R., Mooney, H., Ceballos, G., Young, H. (Eds.), Seasonally Dry Tropical Forests: Ecology and Corservation. Island Press, Washington, DC 20009, USA, pp. 141–156.

MAGAP, 2011. Costos de producción. Ministerio de Agricultura, Ganadería, Acuacultura y Pesca del Ecuador (http://www.magap.gob.ec/sinagap/index.php?option=com_wrapper&view=wrapper&Itemid=97, Accessed 25 Jan 2013).

Mandal, D., Sharda, V.N., 2013. Appraisal of soil erosion risk in the Eastern Himalayan region of India for soil conservation planning. Land Degrad. Dev. 24, 430–437.

Morgan, R.P.C., 2005. Soil erosion and conservation. third ed. Blackwell, Malden.

Morgan, R.P.C., et al., 1998. The European soil erosion model (EUROSEM): documentation and user guide. Silsoe College, Cranfield University.

Nigel, R., Rughooputh, S.D.D.V., 2010a. Soil erosion risk mapping with new datasets: An improved identification and prioritisation of high erosion risk areas. Catena 82, 191–205.

Nigel, R., Rughooputh, S.D.D.V., 2010b. Mapping of monthly soil erosion risk of mainland Mauritius and its aggregation with delineated basins. Geomorphology 114, 101–114.

Ochoa, A., Pineda, L., Crespo, P., Willems, P., 2014. Evaluation of TRMM 3B42 precipitation estimates and WRF retrospective precipitation simulation over the Pacific–Andean region of Ecuador and Peru. Hydrol. Earth Syst. Sci. 18, 3179–3193.

Ochoa-Cueva, P., Fries, A., Montesinos, P., Rodríguez-Díaz, J., Boll, J., 2015. Spatial estimation of soil erosion risk be land-cover change in the Andes of Southern Ecuador. Land Degrad. Dev. 26, 565–573.

Oñate-Valdivieso, F., Bosque, J., 2010. Application of GIS and remote sensing techniques in generation of land use scenarios for hydrological modeling. J. Hydrol. 395, 256–263.

Palacio, R.G., Bisigato, A.J., Bouza, P.J., 2014. Soil erosion in three grazed plant communities in Northeastern Patagonia. Land Degrad. Dev. 25, 594–603.

Panagos, P., Karydas, C., Ballabio, C., Gitas, I., 2014. Seasonal monitoring of soil erosion at regional scale: An application of the G2 model in Crete focusing on agricultural land uses. Int. J. Appl. Earth Obs. Geoinf. 5, 461–487.

Panagos, P., Borrelli, P., Meusburger, C., Alewell, C., Lugato, E., Montanarella, L., 2015. Estimating the soil erosion cover-management factor at European scale. Land Use Policy 48, 38–50.

Pérez-Rodríguez, R., Marques, M.J., Bienes, R., 2007. Spatial variability of the soil erodibility parameters and their relation with the soil map at subgroup level. Sci. Total Environ. 378, 166–173.

Pineda, L., Ntegeka, V., Willems, P., 2013. Rainfall variability related to sea surface temperature anomalies in a Pacific–Andean basin into Ecuador and Peru. Adv. Geosci. 33, 53–62.

Podwojewski, P., Poulenard, J., Zambrana, T., Hofstede, R., 2002. Overgrazing effects on vegetation cover and properties of volcanic ash soil in the páramo of Llangahua and La Esperanza (Tungurahua, Ecuador). Soil Use Manag. 18, 45–55.

Renard, K., Freimund, J., 1994. Using monthly precipitation data to estimate the R-factor RUSLE. J. Hydrol. 157, 287–306.

Renard, K.G., Foster, G.R., Weesies, G.A., McCool, D.K., Yoder, D.C., 1997. Predicting soil erosion by water: a guide to conservation planning with the revised universal soil loss equation. USDA Agriculture Handbook, No. 703 (404 pp.).

Richter, M., Diertl, K.-H., Emck, P., Peters, T., Beck, E., 2009. Reasons for an outstanding plant diversity in the tropical Andes of Southern Ecuador. Landsc. Online 12, 1–35.

Romero, C.C., Baigorria, G.A., Stroosnijder, L., 2007. Changes of erosive rainfall for El Niño and La Niña years in the northern Andean highlands of Peru. Clim. Chang. 85, 343–356.

Ruiz-Sinoga, J.D., Romero-Diaz, A., 2010. Soil degradation factors along a Mediterranean pluviometric gradient in Southern Spain. Geomorphology 118, 359–368.

Savory, A., 1999. Holistic management: a new framework for decision making. second ed. Island Press (616 pp.).

Soil Survey Staff, 1996. Soil survey laboratory methods manual. Soil Survey Investigations Rep. vol. 42. US Dept. Agric.-Nat. Res. Cons. Serv., Washington, DC

Stocking, M., 1981. A working model for the estimation of soil loss suitable for underdevelopment areas. Development Studies Occasional Paper No. 15. University of East Anglia, UK.

Tote, C., et al., 2011. Effect of ENSO events on sediment production in a large coastal basin in northern Peru. Earth Surf. Process. Landf. 36, 1776–1788.

Vázquez, M.A., Larrea, M., Suarez, L., Ojeda, P. (Eds.), 2001. Biodiversidad en los bosques secos del Suroccidente de la provincia de Loja: un reporte de las evaluaciones ecologicas y socioeconomicas rapidas. EcoCiencia, MAE, Herbario Loja y Proyecto Bosque Seco, Quito, Ecuador.

Vrieling, A., Hoedjes, J.C.B., van der Velde, M., 2014. Towards large-scale monitoring of soil erosion in Africa: accounting for the dynamicis of rainfall erosivity. Glob. Planet. Chang. 115, 33–43.

Weber, K.T., Gokhale, B.S., 2011. Effect of grazing on soil-water content in semiarid rangelands of southeast Idaho. J. Arid Environ. 75, 464–470.

Winckell, A., Zebrowski, C., Sourdat, M., 1997a. Los paisajes naturales del Ecuador. Quito, EC, CEDIG, IPGH, ORSTOM, IGM. v. 2 (Geografía Básica del Ecuador). Geografía Física tomo 4 (417 pp.).

Winckell, A., et al., 1997b. Las condiciones del medio natural. Quito, EC, CEDIG, IPGH, ORSTOM, IGM. v. 1 (Geografía Básica del Ecuador). Geografía Física tomo 4 (159 pp.).

Zhang, R., 1997. Determination of soil sortivity and hydraulic conductivity from the disk infiltrometer. Soil Sci. 61, 1024–1030.

Zhao, G., Mu, X., Wen, Z., Wang, F., Gao, P., 2013. Soil erosion, conservation, and eco-environment changes in the Loess Plateau of China. Land Degrad. Dev. 24, 499–510.